LIMNOLOGY and OCEANOGRAPHY

ASLO

Limnol. Oceanogr. 66, 2021, 2141–2158

doi: 10.1002/lno.11733

Fresh and saline submarine groundwater discharge in a large coastal inlet affected by seasonal upwelling

J. Severino P. Ibánhez,[1,2*] **Xosé Antón Álvarez-Salgado**,[2] **Mar Nieto-Cid**,[2,3] **Carlos Rocha**[1]

[1]Biogeochemistry Research Group, School of Natural Sciences, Trinity College Dublin, Dublin, Ireland
[2]Laboratorio de Geoquímica Orgánica, Instituto de Investigacións Mariñas (IIM), Consejo Superior de Investigaciones Científicas (CSIC), Vigo, Spain
[3]Centro Oceanográfico de A Coruña, Instituto Español de Oceanografía (IEO), A Coruña, Spain

Abstract

Submarine groundwater discharge is recognized as a major source of chemicals to the global ocean, exerting large control over coastal water composition. Radon and ^{226}Ra are used to evaluate, for the first time, the occurrence and magnitude of submarine groundwater discharge in the Ría de Vigo, a large, highly productive embayment affected by seasonal, wind-driven upwelling. The system is naturally enriched in ^{222}Rn due to the regional granitic basement geology: high ^{222}Rn activities (up to 10^6 Bq m^{-3}) are detected in wells and boreholes in the drainage basin of the embayment. High ^{222}Rn activities (>400 Bq m^{-3}) are also measured in certain areas of the embayment. Comparatively lower ^{226}Ra activities (<4 10^3 Bq m^{-3}) were measured in the freshwater sources to the bay. Mass balances obtained with a box model are used to perform a volumetric estimate of fresh and saline submarine groundwater discharge in the Ría de Vigo under contrasting circulation patterns. Fresh groundwater is shown to be a relevant hydrological component of the Ria de Vigo water balance, equivalent to 9% ± 4% and 23% ± 9% of the volume discharged by tributary rivers during winter and summer, respectively. On the other hand, recirculation of seawater through permeable sediments is capable of filtering the entire upper volume of the Ria de Vigo through its seafloor in <100 days and might thus be a previously overlooked major source of regenerated solutes to the system.

The transport of water from the sediments to the overlying water regardless of its origin and composition is called submarine groundwater discharge (Burnett et al. 2003). Therefore, submarine groundwater discharge includes both fresh continental groundwater and seawater recirculated through marine sediments. Fresh submarine groundwater discharge usually occurs nearshore, whenever a coastal aquifer is hydraulically connected to the sea and a positive head gradient exists with the ocean (Johannes 1980). Nevertheless, at a global scale, seawater recirculation through permeable beds is the primary component of submarine groundwater discharge and is largely driven by density gradients and the interaction of currents, waves, or tides with marine permeable sediments and bedforms (Boudreau et al. 2001; Wilson 2005; Santos et al. 2012).

While fluvial inputs to the coastal zone are well constrained, thus allowing relatively accurate estimates of solute loads to the coastal ocean, the identification and quantification of submarine groundwater discharge is difficult due to its commonly diffuse spread within the receiving coastal system. The use of radioisotope tracer techniques partially unveiled the geographical ubiquity and magnitude of submarine groundwater discharge at a global scale, essentially during the last decade. Recent estimates indicate submarine groundwater discharge is a large source of water (Kwon et al. 2014) and major nutrients (Cho et al. 2018) to the global ocean. Nevertheless, the relative contribution of fresh submarine groundwater discharge to total submarine groundwater discharge is still highly uncertain, in spite of recent attempts to provide a comprehensive global appraisal of this freshwater input to the oceans (Zhou et al. 2019; Luijendijk et al. 2020). Although the global significance of fresh submarine groundwater discharge is not well-constrained, it is clear that it is a highly variable freshwater source to the sea that can be important at the regional and local scales. This mode of submarine groundwater discharge is particularly important because it drives the

*Correspondence: pinoibaj@tcd.ie

Author Contribution Statement: J.S.P.I., X.A.A.-S., and C.R. conceived and designed the study. J.S.P.I. and M.N.-C. performed the setup, sampling and analysis of samples. J.S.P.I. performed data analysis with contributions from X.A.A.-S. and C.R. J.S.P.I. wrote the first version of the manuscript and all authors contributed to and approved the final text.

hidden transport of solutes originated from land and directly links human land use with coastal resilience. Fresh submarine groundwater discharge has been already identified as a major source of nutrients and pollutants to coastal ecosystems (e.g., Leote et al. 2008; Welch et al. 2019), with direct impacts over their ecology and resilience (Moore 2010; Taniguchi et al. 2019).

Here, we evaluate, for the first time, submarine groundwater discharge into the Ría de Vigo (NW Iberian Peninsula), a complex, highly productive coastal inlet subject to seasonal upwelling that supports primary production of major ecological and economic significance (Figueiras et al. 2002). Relying on the disproportionate importance of upwelling in fertilizing the embayment, other sources of solutes to the system have received less attention. Nevertheless, previous studies have shown that submarine groundwater discharge can be an important component of the hydrology and fertilization of upwelling ecosystems (e.g., Lecher et al. 2015; Luo et al. 2018). Different to other upwelling ecosystems, the changing wind direction characteristic of the latitudes of the study site (~42°N) drives the short-term alternation of upwelling and downwelling events that dramatically modify the water circulation patterns in the embayment (Álvarez-Salgado et al. 2000; Gilcoto et al. 2017). Thus, we couple the use of radioisotope tracers with explicit estimates of water circulation in the embayment to quantify the magnitude of submarine groundwater discharge. Furthermore, we follow a multi-tracer approach (^{222}Rn and ^{226}Ra) to estimate the relative contribution of fresh and saline submarine groundwater discharge.

Methods

Study site: Hydrography and dynamics

The Ría de Vigo is a large, semi-enclosed embayment (176 km^2) in the NW Iberian Peninsula (Fig. 1). Located at the northern limit of the Canary current eastern boundary upwelling ecosystem, nutrient-rich Eastern North Atlantic Central Water is transported from about 150–200 m in the adjacent ocean to the surface layer in the coast during the spring and summer (Arístegui et al. 2009). This, together with the intricate orography of the Galician coast, makes this area the most productive European marine ecosystem per square meter in terms of exploitation of living resources. The system of coastal inlets of the Galician coast, to which the Ría de Vigo belongs, yielded about 54% of the European mussel production in 2017 (265,000 metric tons), billing 130 million Euro and supporting 11,000 direct and 9000 indirect employees (FAO 2018; Labarta and Fernández-Reiriz 2019).

The Ría de Vigo comprises a large shallow area in the NE (San Simón Bay, <7 m depth) and depth then varies, up to 55 m depth at the southern mouth of the embayment (Fig. 1). San Simón Bay is connected to the middle segment of the embayment through a narrow channel (Rande Strait, 600 m width), while exchange with adjacent shelf waters is partially limited by the Cíes Islands (Fig. 1). The embayment is mesotidal, with an average tidal amplitude of 2.2 m. Climate in the region is oceanic, with average temperatures of ~ 15°C, although there is a large gradient in air temperature, wind speed, evapotranspiration and precipitation from the littoral zone to the mountainous inland (Raposo et al. 2012). Precipitation is mainly concentrated during autumn and winter and can vary from ~ 900 mm in the Cíes Islands to ~ 2500 mm at the innermost part of the basin.

The main drivers of water circulation in the Ría de Vigo are river discharge and coastal winds. Only the inner part of the embayment shows a purely positive estuarine circulation pattern forced by continental runoff, whereas, in the outer part, Ekman transport over the continental shelf controls the subtidal circulation (Álvarez-Salgado et al. 2000). Northerly winds that prevail during spring and summer promote upwelling and thus enhance the positive residual circulation pattern, while during autumn and winter the dominant southerly winds produce downwelling of shelf surface waters, inducing a reversal of the positive circulation in the outer part of the embayment (Arístegui et al. 2009). Local winds further reinforce the prevailing circulation patterns by reducing the friction between vertical layers flowing in opposite directions (Gilcoto et al. 2017). Subtidal circulation shows a quick response time to wind forcing (<15 h), explained by the narrowness, equatorial orientation, vertical stratification and depth of the embayment (Gilcoto et al. 2017). Furthermore, sporadic intrusions of the Minho river plume can significantly alter water exchange with the adjacent shelf (Des et al. 2019).

Coastal upwelling is the main allochthonous nutrient source to the Ría de Vigo. Considering surface sediments in the embayment as an external source, Fernández et al. (2016) estimates that upwelling represents 58% of the inorganic nitrogen input to the embayment. Benthic nutrient regeneration is suggested to account for 23% of the inorganic nitrogen available in the Ría de Vigo, sewage 17% and riverine and atmospheric inputs account for 2% (Fernández et al. 2016).

Study site: Geological and hydrogeological setting

The Ría de Vigo is a drowned fluvial valley incised on Paleozoic meta-sedimentary and granite basement rocks that largely dominate the area following the dominant NE–SW trending faults (Fig. 1). Sedimentary deposits are relatively young and originated from the last rise in sea-level (García-García et al. 2005). Two lithological units overlay the weathered granite basement: a siliciclastic alluvial deposit of variable thickness (up to 3 m) dominated by silty muds with sand, silty gravels and coarse sand, on which an expansive unit composed by marine bioclastic sands and muds heterogeneously distributed and with variable thickness (8.0–3.2 m) sits (García-García et al. 2005). Surface sediments are dominated by lime muds within the inner and central segments of the embayment, whereas sands and gravels dominate the outer, more energetic, segment (Vilas et al. 2005).

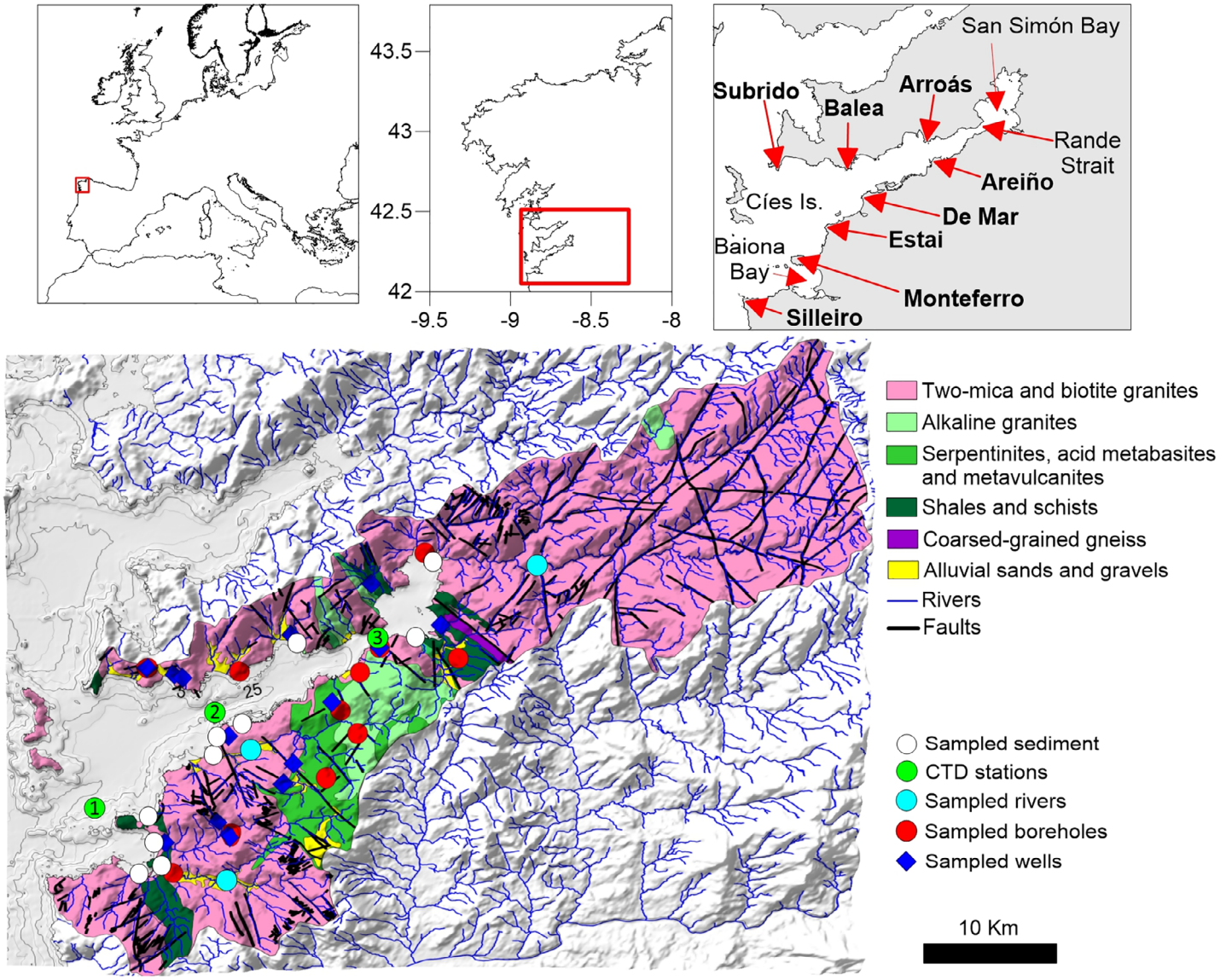

Fig 1. Study site (Ría de Vigo, NW Iberian Peninsula) showing the drainage basin, dominant geological composition (adapted from IGME 2003), faults and rivers, along with sediment and continental water sampling locations and CTD stations: 1. South Mouth; 2. Central Station; 3. Rande. The main geographical features (capes and cape points in bold, straits, bays, and islands) are also shown in the top right map, indicated by arrows.

The Ría de Vigo drains a watershed of 709 km^2 dominated by Paleozoic alkaline and calc-alkaline granitic and metamorphic (schist and gneiss) basement rocks that regularly reach the soil surface (Fig. 1). Only small quaternary deposits associated to alluvial transport are present (Fig. 1). Both types of bedrock have traditionally been considered of low permeabilities (Gustafson and Krásný 1994). Adding to the preferential NE–SW direction, NW–SE and N–S trending faults are also present in the basin (Fig. 1), giving the basement rocks some secondary permeability and groundwater storage capacity. The hydrogeology of the area can be described conceptually as a two-layer aquifer, given the distinctive groundwater flow patterns: a shallow unit contained within the regolith and the highly weathered uppermost part of the basement rocks, and an underlying unit delimited by the fractured bedrock (Raposo et al. 2012). Below these, the basement rock is considered essentially impermeable. The surface aquifer has a variable thickness of up to 20 m as observed in lithological logs of wells and geophysical studies in the vicinity of the study site (Mota et al. 2004; Ramalho et al. 2012). This surface aquifer is characterized by high permeabilities and strong phreatic level fluctuations associated with short residence times. Water levels are highly dependent on rainfall recharge (Raposo et al. 2013). This section commonly shows large horizontal flow transfer that follows the local topography and provides most of the groundwater storage capacity in crystalline

aquifers of the region (Mota et al. 2004; Ramalho et al. 2012; Raposo et al. 2012). Underneath, the fractured rock aquifer has also a highly variable thickness—up to 100 m—but lower storage capacity and groundwater flow compared to the overlying aquifer (Raposo et al. 2012). Storage in the local crystalline aquifers is nevertheless very heterogeneous, highly dependent on the magnitude and direction of the fractures (Mota et al. 2004; Raposo et al. 2012).

Sampling strategy in waters of the Ría de Vigo

Surface water samples (0.5 m depth) of the Ría de Vigo were collected during winter (28th of February and 5th of March) and summer (29th, 30th, and 31st of August) 2018 covering its entire shoreline. These samples were collected by boat with Niskin bottles and transferred to air-tight glass bottles (250 mL) for subsequent radon (^{222}Rn) and radium (^{226}Ra) determinations in the laboratory. During winter and summer, a total of 41 and 49 surface water samples respectively were collected, with an average spatial interval of 1027 and 1155 m. During the summer survey, additional water samples were collected at three points throughout the water column to evaluate the distribution of ^{222}Rn and ^{226}Ra activities with depth. Sampling lasted for ~4 h centered around low tide during spring tides to minimize tidal water transport influence over the surface distribution of target solutes. Upon arrival in the lab, a Durridge RAD7 radon detector with a RADH2O accessory (Durridge Company) was used to determine ^{222}Rn activities in the collected water samples within 2 days of sampling. Corrections for internal ^{222}Rn decay for the time elapsed since collection until the moment of analysis were applied. The air-purged samples were subsequently stored in hermetically closed bottles for a minimum of 30 days (i.e., more than 5 times the ^{222}Rn half-life) to allow secular equilibrium to develop between ^{222}Rn ingrowth and ^{226}Ra in water. The in-water ^{226}Ra activity was then determined as the ^{222}Rn activity measured in these aged samples. Samples were analyzed with the standard WAT250 protocol included with the equipment (30-min counting cycle; Durridge RAD7 manual). In between determinations, the internal volume of the radon monitor was intensively purged by recirculation through an activated carbon ^{222}Rn trap until zero background ^{222}Rn activity was achieved in internal loop. The detection limit, precision, and accuracy of our procedure is 36 Bq m^{-3}, 12 Bq m^{-3}, and 91%, respectively, determined from the analysis of regular blanks made with ^{222}Rn-free water (n = 36). In-water excess ^{222}Rn activity, i.e., unsupported by ingrowth from ^{226}Ra decay, was then taken as the difference between the ^{222}Rn activities measured initially and the ^{226}Ra activity determined in the aged samples.

The properties of the water column during February/March 2018 were described using vertical profiles of water temperature, salinity and pressure measured by the Galician Monitoring Program (INTECMAR; www.intecmar.gal) on the 27th of February, with surface water temperature measured with a Seabird SBE 27 CTD in complement. For August 2018, vertical temperature, salinity and pressure profiles were obtained with a RBRconcerto CTD and the Seabird SBE 27 CTD was coupled to the continuous water intake on board to continuously record temperature and salinity in the embayment's surface. During both surveys, aliquots from the sampling stream were taken at each sampling station for laboratory determination of salinity with a Guildline Portasal salinometer.

Complementary measurements

Supplementary water samples were collected from the main rivers discharging into the embayment (Fig. 1). These samples were collected within 2 weeks of the surveys in the embayment. Additional groundwater samples were collected in the area surrounding the Ría de Vigo during two basin-wide sampling surveys performed from the 12th of February to the 4th of May 2018 and from the 6th of September to the 4th of October 2018. During these, groundwater samples were collected from 12 wells and 15 boreholes (Fig. 1). In-water ^{222}Rn and ^{226}Ra activities in these samples were determined as already described. During winter, limited ^{226}Ra determinations in groundwaters were performed. Due to the high ^{222}Rn levels found in groundwater samples, dilution with ^{222}Rn-free water was performed prior to analysis. Atmospheric ^{222}Rn activities in the Ría de Vigo were determined on land (42.226019° N, 8.752203° W) within 2–4 days of the surface water surveys.

To estimate groundwater ^{222}Rn equilibrium activities, a multi-pronged approach was followed: muddy sediment from different locations along the embayment (n = 4) was sampled with mini-coring devices (10 cm length, 2.5 cm diameter) and transferred to air-tight glass bottles pre-filled with ^{222}Rn-free water. Radon activities were measured in the resulting slurry following homogenization. The embayment's sands were also sampled (n = 3) and slurry-equilibration experiments performed following Colbert and Hammond (2008). For completion, sandy sediment groundwater ^{222}Rn activities were also measured directly: groundwater was collected from the lower intertidal of different locations (n = 6) at a depth of 86 cm into the sand with push-pull piezometers. Dissolved ^{226}Ra in shore groundwaters of the Ría de Vigo were determined after allowing samples to reach secular equilibrium between ^{222}Rn and ^{226}Ra and following the same procedure as for the embayment samples. Radon activities determined in sandy and muddy sediment porewaters were similar (1697 ± 303 and 1345 ± 281 Bq m^{-3}, respectively). Based on this, for diffusive ^{226}Ra flux calculations, muddy sediments were assumed to have the same dissolved ^{226}Ra levels as determined in the sandy groundwater samples. Sediment and groundwater sampling sites are shown in Fig. 1.

Radioisotope mass balance approach in surface waters of the Ría de Vigo

To find whether submarine groundwater discharge is a significant source of radionuclides to the Ría de Vigo, we

developed ^{222}Rn and ^{226}Ra mass balances for both survey periods. Circulation (advective fluxes) was described using the specific parametrization for the Ría de Vigo developed by Álvarez-Salgado et al. (2000). They obtained non-steady-state horizontal and vertical exchange fluxes for the boundaries of a box model and found significant relationships with upwelling intensity (offshore Ekman transport) and continental runoff, explaining 95% of exchange fluxes between the boxes. We followed their approach and divided the embayment into three boxes. Each box consists of two superimposed water layers flowing in opposite directions. The shallower inner box that corresponds to San Simón Bay (Fig. 1) was included as a single layer compartment. In the two outer boxes, the depth at which the vertical distribution of density equals the average density of the water column, i.e., the center of gravity, was used as the boundary between the two superimposed water layers in the embayment (Rosón et al. 1997). To use the advective flux parametrization of Álvarez-Salgado et al. (2000), offshore Ekman transport is obtained from the Instituto Español de Oceanografía (http://www.indicedeafloramiento.ieo.es) at 43°N 11°W using winds derived from sea level pressure field over the ocean supplied by the U.S. Navy's Fleet Numerical Meteorology and Oceanography Centre model. Specifically, the cross-shore component of the upwelling index (UI_x), in m^3 per m of coastline per second, is calculated after Bakun (1973):

$$UI_x = \frac{\rho_a C_d |V| V_y}{\rho_w f} \quad (1)$$

where ρ_a is the density of air, C_d is an empirical drag coefficient, $|V|$ and V_y are the daily module and north component of the geostrophic winds, ρ_w is the density of seawater and f is the Coriolis parameter. The average upwelling index registered during the 3 days prior each sampling date was used for the calculations (Álvarez-Salgado et al. 2000). Calculated horizontal fluxes were $-9.48 \pm 1.30 \times 10^3$ m^3 s^{-1} between Box 3 and the open ocean and $-1.65 \pm 0.02 \times 10^3$ m^3 s^{-1} between Boxes 2 and 3 during the winter survey. Negative values indicate downwelling conditions. During the summer survey, under upwelling conditions, horizontal fluxes of $9.93 \pm 1.57 \times 10^3$ m^3 s^{-1} between Box 3 and the open ocean and $2.77 \pm 0.25 \times 10^3$ m^3 s^{-1} between Boxes 2 and 3 were obtained. Advective exchanges between Boxes 1 and 2 and vertical turbulent vertical mixing fluxes in the outer boxes of the embayment (not parametrized) were taken from those presented in Álvarez-Salgado et al. (2000). Specifically, these authors determined exchange fluxes in five different periods of contrasting circulation within the embayment. A spring downwelling event (-6.00×10^3 m^3 s^{-1} between Box 3 and the open ocean, -0.74×10^3 m^3 s^{-1} between Boxes 2 and 3 and 0.3×10^3 m^3 s^{-1} between Boxes 2 and 1, with turbulent fluxes of 1.08 m^3 s^{-1} in Box 3 and 0.89 m^3 s^{-1} in Box 2) and a winter upwelling event (7.63×10^3 m^3 s^{-1} between Box 3 and the open ocean, 1.70×10^3 m^3 s^{-1} between Boxes 2 and 3 and 0.3×10^3 m^3 s^{-1} between Boxes 2 and 1, with turbulent fluxes of 1.14 m^3 s^{-1} in Box 3 and 0.35 m^3 s^{-1} in Box 2) are the surveys with advective fluxes closer to those calculated here for winter and summer, respectively. Accordingly, the remaining unknown exchange fluxes were taken from these surveys in Álvarez-Salgado et al. (2000).

Closing the mass balances of excess ^{222}Rn (hereafter referred as ^{222}Rn) and ^{226}Ra requires the calculation of inventories, i.e., vertically integrated quantities, of both radionuclides. First, measured activities were linearly interpolated into a regular grid of 500×500 m resolution. As in Box 3, we lack coverage of some central portions of the embayment, extrapolation of the activities from each measured point was permitted to a radius equivalent to the mean distance among measured points (~1.2 km for both surveys). Then, the inventories were calculated by multiplying the gridded activities by the mean water layer depth for each grid cell (i.e., for the surface water layer, either the vertical depth to the center of gravity or the actual depth when shallower than the center of gravity) using a high-resolution bathymetric map of the embayment. Spatially averaged inventories were then used together with calculated advective transport fluxes to obtain the advective transport of each radionuclide at each box boundary. Mass balances were then constructed for each box as follows:

$$\frac{dI_{\text{box}}}{dt} = F_{\text{advective}} + F_{\text{turb}} - F_{\text{sea-air}} + F_{\text{river}} + F_{\text{dif}} - F_{\text{decay}} + F_{\text{SGD}} \quad (2)$$

where I_{box} is the inventory at each box, $F_{\text{advective}}$ are the advective lateral and vertical fluxes of radionuclides across each box and water layer limits, F_{turb} is the turbulent vertical flux at each box, $F_{\text{sea-air}}$ is the degassing flux of ^{222}Rn to the atmosphere, F_{river} is the radionuclide transport by rivers, F_{dif} is the diffusive flux of each radionuclide across the sediment–water interface and across the vertical limits of the two water layers at each box, F_{decay} is the decay of each radionuclide and F_{SGD} is the radionuclide flux associated to submarine groundwater discharge.

$F_{\text{sea-air}}$ was calculated using the gridded surface water ^{222}Rn activities and measured atmospheric ^{222}Rn activities using the gas flux model of MacIntyre et al. (1995):

$$F_{\text{sea-air}} = (\text{Rn}_{\text{sea}} - k * \text{Rn}_{\text{air}}) * K \quad (3)$$

where Rn_{sea} is the gridded surface water ^{222}Rn activity, Rn_{air} is the measured atmospheric ^{222}Rn activity, k is the ^{222}Rn partitioning coefficient, and K is the gas transfer coefficient. K was calculated after MacIntyre et al. (1995) using the wind speed at 10 m obtained from the meteorological stations available from Meteogalicia (www.meteogalicia.gal). Due to the large land-to-ocean gradient of wind speed characteristic of the study area, the meteorological stations of Cíes Islands (42.2118°N, 8.90842°W), Vigo (42.2259°N, 8.7135°W), and Redondela (42.3207°N, 8.60187°W) were used for the calculation of K for the outer, middle, and inner boxes, respectively. As for the calculation of

advective transport, the average wind speed registered during the 3 days prior to each sampling date was used for the calculation of K and thus, $F_{sea-air}$. A k for each box was calculated as a function of temperature and salinity following Schubert et al. (2012), using the average of the temperature and salinity measured in surface waters within the boundaries of each box for each survey. F_{river} was calculated from the measured activities in river water and the river discharge. The latter were obtained from the public gauge stations available from Aguas de Galicia (https://augasdegalicia.xunta.gal). For those rivers where the gauging station is far from the mouth (e.g., Verdugo-Oitavén, Lagares), recorded discharges were extrapolated to the river mouth based on the ratio between the total and the monitored area of the river basin. The discharge of ungauged rivers into the system was estimated from daily rainfall rates following the parametrization of Ríos et al. (1992), specific for the Ría de Vigo basin. The daily river discharges were then averaged as for the period used in the upwelling index calculation (i.e., from 3 days prior to each day of sampling). Radon and ^{226}Ra activity in those smaller rivers were taken as the average of the activities measured in the sampled rivers. F_{dif} was calculated from the averaged equilibrium saline groundwater ^{222}Rn and ^{226}Ra activities and gridded surface water ^{222}Rn and ^{226}Ra activities following Martens et al. (1980). Finally, F_{decay} was calculated with the gridded inventories using the respective decay constants. A graphical overview of the box discrimination within the embayment and processes considered in our mass balances is shown in Fig. 2.

This budgeting exercise was restricted to the surface water layers of each box, where most of our determinations were performed. Steady state was assumed for radionuclide inventories (i.e., $\frac{dI_{box}}{dt} = 0$), to solve Eq. 2 for F_{SGD}. We lack radioisotope determinations in depth for the winter survey. However, while this data is important during upwelling conditions, as there is significant advective transport from the deeper water layers to the surface (Fig. 2), it would only affect the estimation of the turbulent mixing flux during downwelling conditions. Thus, turbulent mixing was not considered for the mass balances during the winter survey.

Estimation of uncertainty

The uncertainty associated with calculated inventories and spatially averaged activities of ^{222}Rn and ^{226}Ra was estimated using a Monte Carlo approach. We calculated 100 inventories following the gridded method explained before with radionuclide activities drawn randomly from their probability distributions. The standard deviation resulting from the Monte Carlo simulations was considered to represent the error associated with our calculated inventories and mean activities. Additional uncertainty terms are associated with the advective and turbulent mixing fluxes, as well as the ^{222}Rn degassing flux. The uncertainty associated with the advective water fluxes within the box model was estimated directly from the parametrizations of Álvarez-Salgado et al. (2000), which allow estimation of the uncertainty associated with each individual advective flow rate. An uncertainty of 25% was assigned to transport values obtained from the literature (i.e., lateral flux from Box 1 to Box 2 and vertical turbulent fluxes). The uncertainty associated with the sea-air ^{222}Rn degassing flux rate

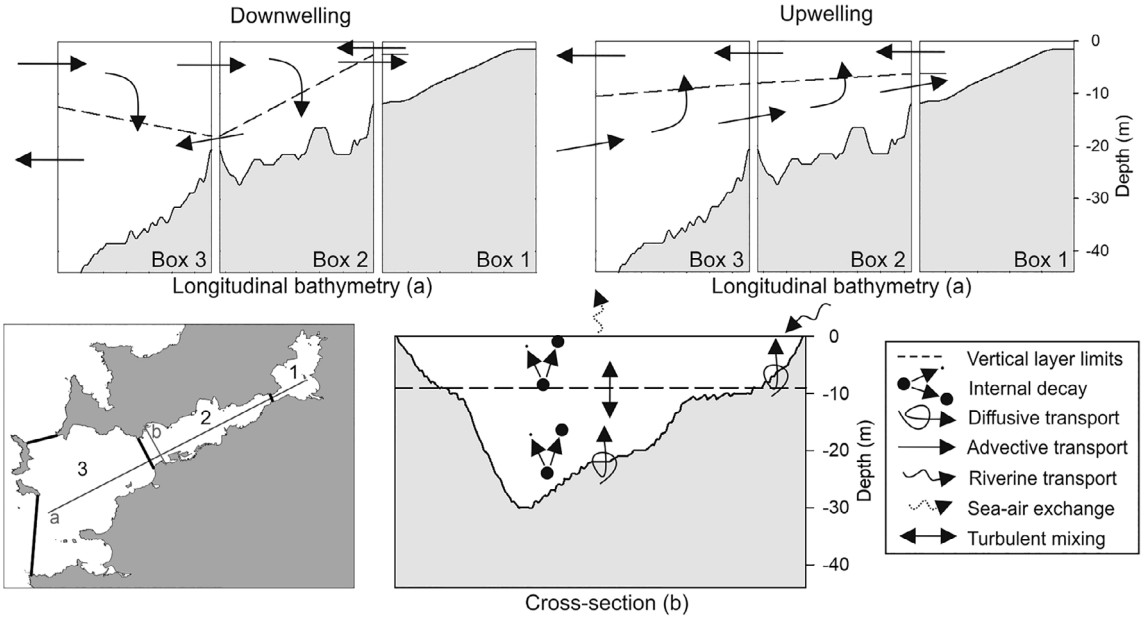

Fig 2. Schematic view of the main processes included in the mass balances of ^{222}Rn in excess and ^{226}Ra in the Ría de Vigo. Longitudinal (**a**) and transversal (**b**) bathymetric sections of the embayment are included. Processes included in the mass balances other than advection are shown in the transversal section scheme (b).

estimates following MacIntyre et al. (1995) is 34%. These uncertainties were then propagated throughout all calculations by applying general rules of end-to-end propagation of error (Taylor 1997).

Results

Hydrographic conditions

The two sampling periods are representative of contrasting downwelling/upwelling conditions in the Ría de Vigo (Figs. 3, 4). Downwelling, forced by southerly winds, dominated during the winter survey as expected from the negative value of the upwelling index (Fig. 3). A short northerly wind event that promoted a reversal of the circulation pattern toward weak upwelling was observed in between the two sampling dates. This became apparent in the accumulated residual seawater flux calculated for the winter sampling period (Fig. 4a). Positive residual seawater flux signals seawater entering the embayment though the deep layer (i.e., upwelling), and the weak upwelling event occurring between the sampling days reversed the accumulated residual seawater flux. Nevertheless, this pulse was not enough to renew the volume of the embayment (Fig. 4a) and net downwelling conditions (negative accumulated residual seawater flux) dominated throughout sampling. This period was also accompanied by significant rainfall and river discharge (Figs. 3, 4c). During downwelling conditions, shelf surface waters are transported onshore by Ekman transport, entering the embayment along the surface layers and developing a convergence front with the offshore transport promoted by continental runoff. This detail is observable in the vertical CTD profiles measured on the 27th of February 2018 inside the embayment (Fig. 5; *see* Fig. 1 for sampling locations). A stratified water column is observable throughout the embayment mainly caused by salinity gradients, with a much deeper surface water mixed layer at the central station (>15 m depth), where the convergence between the opposite outer and inner flows occurs, compared to the Southern mouth (<10 m depth; Fig. 5).

The summer survey captured stable upwelling conditions alongside minimum riverine discharge (Figs. 3, 4b). The water column was stratified throughout the embayment. Upwelled shelf bottom waters could be observed in the deeper layers, inducing much cooler temperatures than those found at the surface. The depth of the surface mixed layer inside the embayment was never deeper than 10 m during this survey (Fig. 5). Also as expected, the surveys highlighted the strong seasonality in sea surface temperature and sea surface salinity within the Ría de Vigo (Fig. 6). Differences of up to 8°C in temperature and five salinity units were found between winter and summer, with cooler temperatures and lower salinities in winter. The lowest salinities during winter were found in San Simón Bay, the innermost and shallowest part of the embayment and where the main river system discharges (River Verdugo-Oitavén; Fig. 1). Salinities lower than 35 were found throughout the embayment during this survey. In contrast, during summer the lowest salinity measured in the discrete samples was 34.5, measured in the Baiona and San Simón Bays (Fig. 6; *see* Fig. 1 for the location of both bays). A fresher area, located in the North-East part of the embayment between Rande Strait and Arroás Point, was also highlighted by the continuous measurements with the lowest salinities recorded during summer, although this was not captured by the discrete samples.

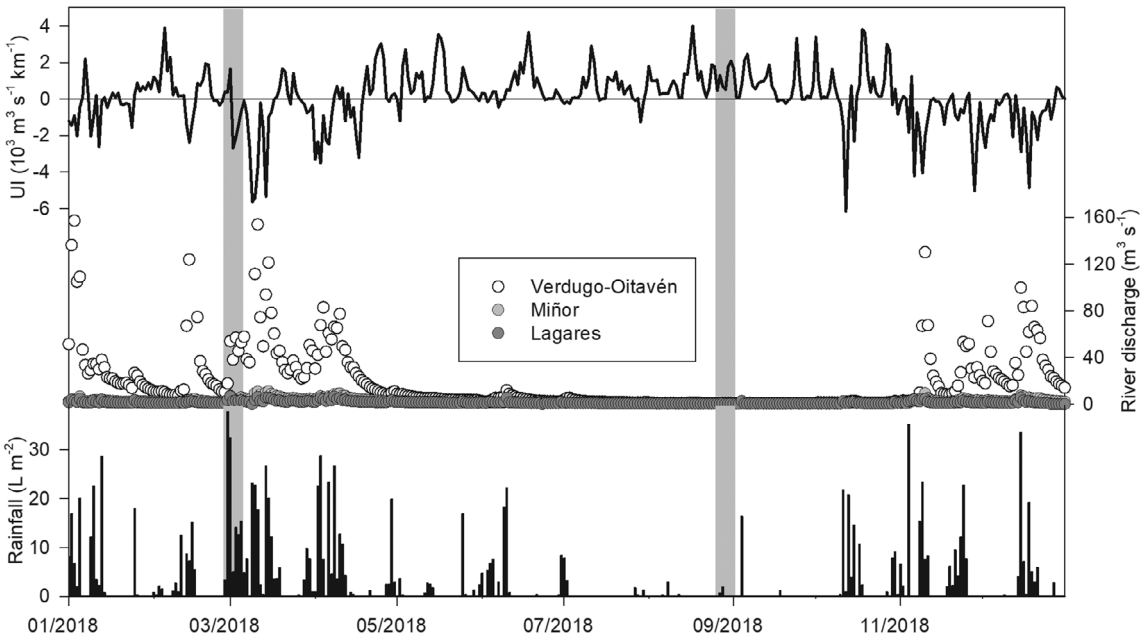

Fig 3. Daily upwelling index (**a**), discharge of the main rivers of the system (**b**), and rainfall (**c**). Sampling dates are shown with vertical gray bars.

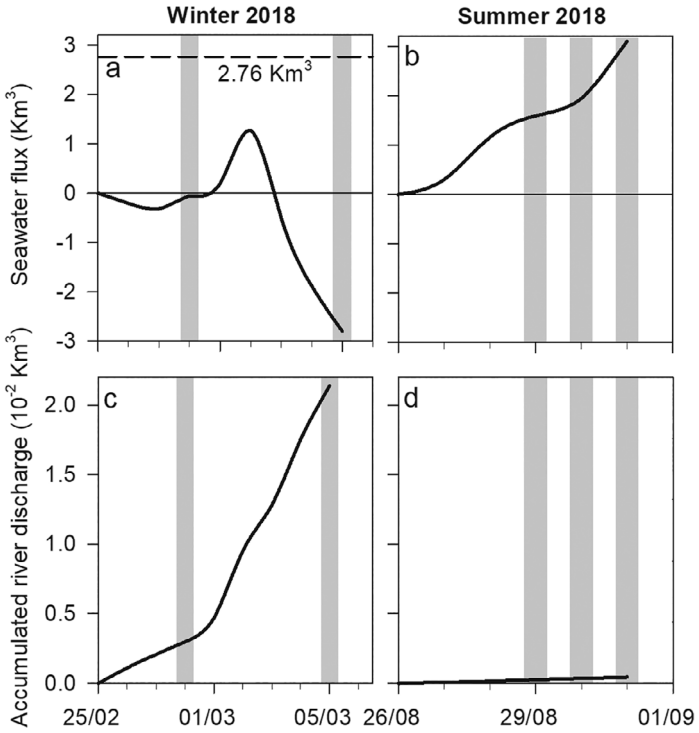

Fig 4. Accumulated residual seawater flux (**a**, **b**) and river discharge (**c**, **d**) for each survey. The accumulation of seawater flux at the mouth of the embayment and total river discharge are displayed, from a starting point 3 days prior to the first day of sampling. Positive residual seawater flux denotes seawater entering the embayment through the bottom water layer (upwelling). The days of sampling are shown as vertical gray bars. The 2.76 km^3 threshold shown marks the volume of the Ría de Vigo.

Distribution of in-water ^{226}Ra and ^{222}Rn in the Ría de Vigo

Surface waters of the Ría de Vigo were characterized by high and spatially variable ^{222}Rn and ^{226}Ra activities. In any survey, the higher ^{222}Rn activities were measured in the inner parts of the embayment, particularly in San Simón Bay and near Arroás point (Fig. 7a,b). Radon activities were comparatively large in summer and winter notwithstanding the much higher surface salinity measured throughout the embayment in summer. Peak ^{222}Rn in-water activities of 515 ± 42 and 483 ± 82 Bq m^{-3} were recorded during February and August, respectively. In the outer part of the embayment, ^{222}Rn activities surpassed 250 Bq m^{-3} in Baiona Bay (not sampled during February). On the other hand, concurrent ^{226}Ra activities show a contrasting spatial distribution between both surveys (Fig. 7c,d): in February, the highest ^{226}Ra activities were found in the outer part of the embayment, while during August, they were found primarily in the inner part, with levels as high as 359 ± 62 Bq m^{-3} recorded inside San Simón Bay.

The vertical distribution of ^{226}Ra and ^{222}Rn activities were also measured during summer at the stations where vertical CTD profiles were taken (Fig. 5, lower panels). The existence

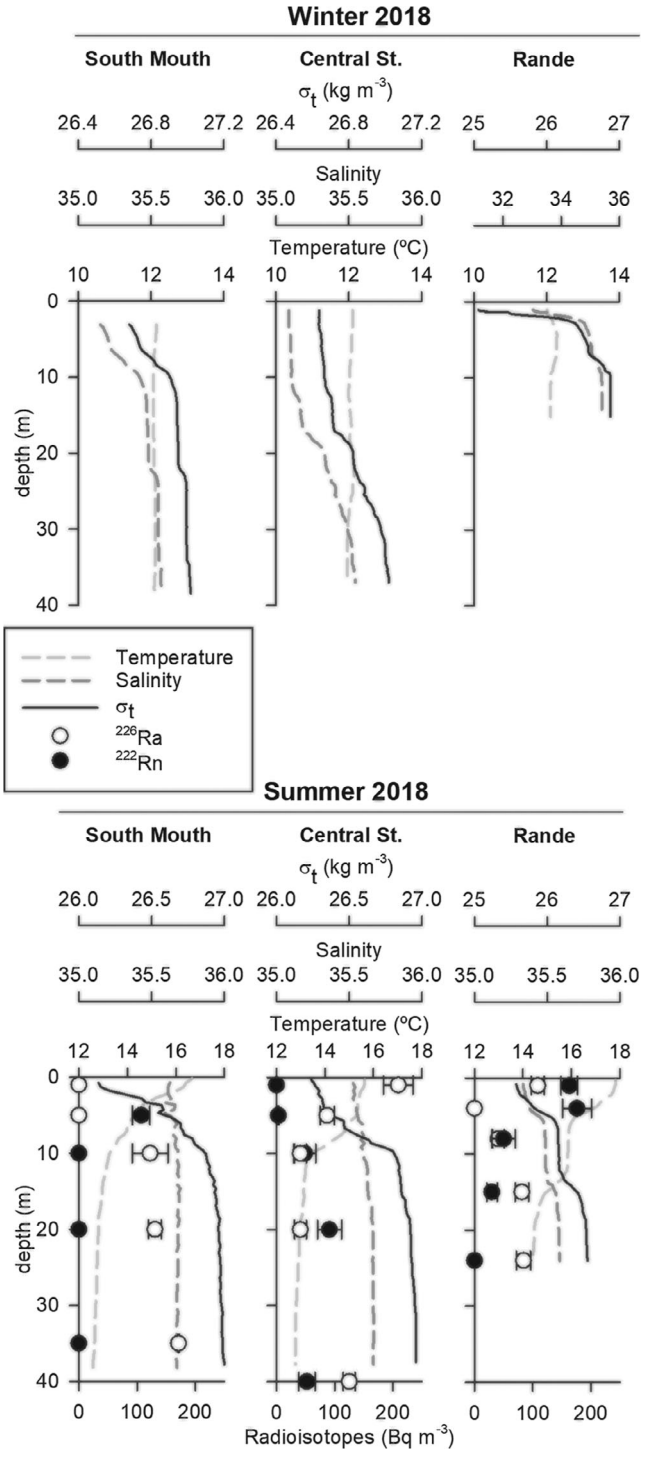

Fig 5. Vertical CTD profiles obtained from the Galician Monitoring Program (INTECMAR; www.intecmar.gal) on the 27th of February 2018 (upper panels) and those measured during the survey performed during the summer 2018 (lower panels). σ_t refers to the density of water-1000. Additionally, ^{222}Rn in excess and ^{226}Ra activities measured along the water column at each location during the summer survey are also shown. The location of the three sampling stations are shown in Fig. 1.

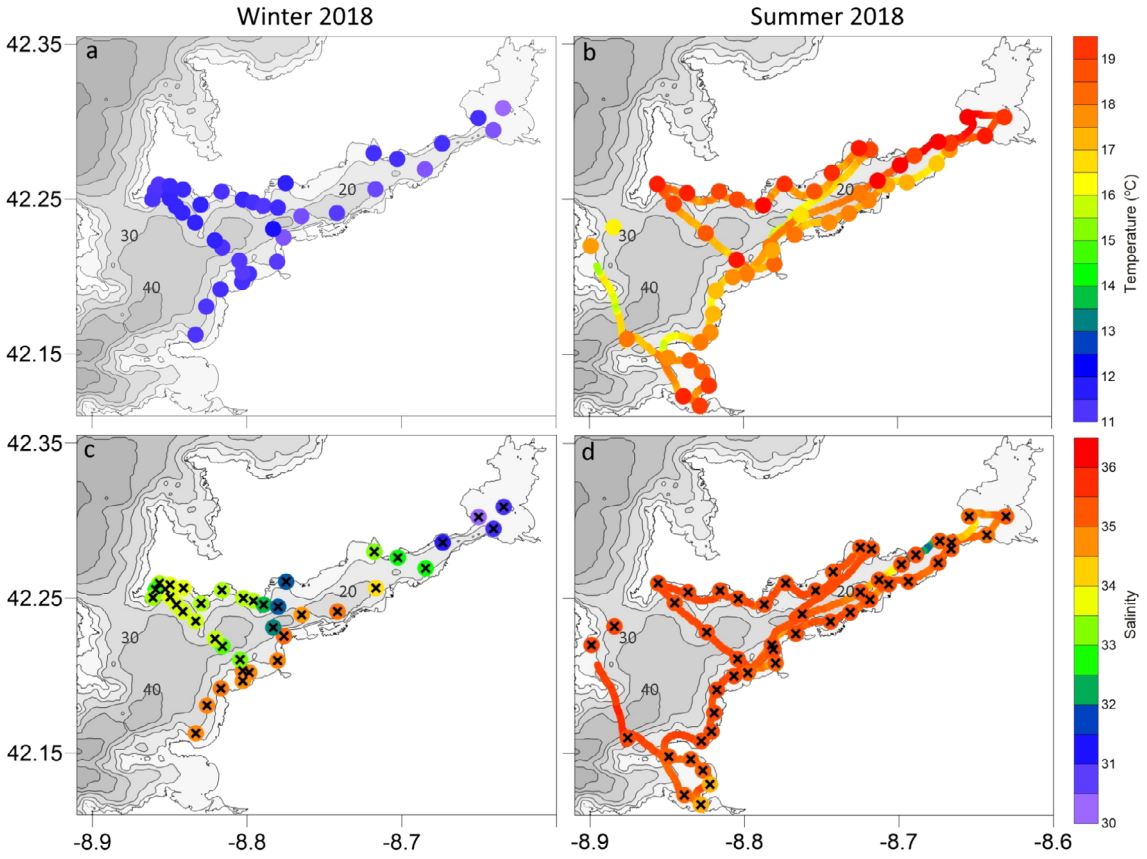

Fig 6. Spatial distribution of measured temperature (upper panels) and salinity (lower panels) in surface waters of the Ría de Vigo during winter and summer 2018. Additionally, continuous temperature and salinity measurements in surface waters are also shown for the summer survey. The location of the sampling points for radioisotopes is also shown using cross symbols in the lower panels. Bathymetric labels are shown in meters.

of two distinct layers could be inferred from the three profiles. With the exception of the central station, ^{222}Rn activities peaked in the surface water layer and then decreased to almost homogeneous values below the pycnocline. Radium on the other hand shows the opposite pattern, with higher activities generally found at depth. During upwelling conditions, shelf waters enter the embayment along the seafloor. The vertical distribution of radioisotopes at the southern mouth found in August shows the adjacent shelf sea to be a source of ^{226}Ra to the embayment (122 ± 32 Bq m^{-3}). This incoming water mass is not a source of ^{222}Rn as none is found in the entire deep-water layer. By contrast, in Rande strait, the surface water layer transported significant ^{222}Rn quantities out of San Simón bay toward the East (169 ± 29 Bq m^{-3}), even if riverine inputs into the system were low during this period.

Radon and radium in continental waters

Continental waters in the Ría de Vigo basin show very high ^{222}Rn activities (Table 1; Fig. 8). Radon activities measured in the three rivers exceeded 1.2 10^3 Bq m^{-3}, with the lowest registered in the Verdugo-Oitavén, the largest of the trio. Radon activities in groundwater are at least one order of magnitude higher than in surface waters, with high variability (Fig. 8). The main factor determining groundwater ^{222}Rn levels at the study site was screening depth within the aquifer. Samples taken from wells dug into the regolith (average well depth 11.3 m, range: 8–17 m depth; n = 12) showed ^{222}Rn activities that ranged from 8.0 ± 0.5 10^3 Bq m^{-3} in February in Alcabre near Cape de Mar, to 393 ± 2 10^3 Bq m^{-3} in August in Nerga, near Cape Subrido (Fig. 1). The Alcabre well that had the lowest ^{222}Rn activities is mostly used for irrigation and thus water extraction is minimal during February. The ^{222}Rn activities recorded in February there may therefore be unrepresentative of actual groundwater levels due to the expected high ^{222}Rn loss from the stagnant well water by decay and evasion. Radon activities measured in groundwater samples taken from boreholes screened at the level of the fractured rock unit (average borehole depth 44.5 m, range: 28–80 m depth; maximum salinity recorded: 0.08; n = 15) were much higher. The upper range of activities, three orders of magnitude higher than those found in surface waters, were recorded in Nerga in August (2738 ± 67 10^3 Bq m^{-3}). Groundwater ^{222}Rn levels

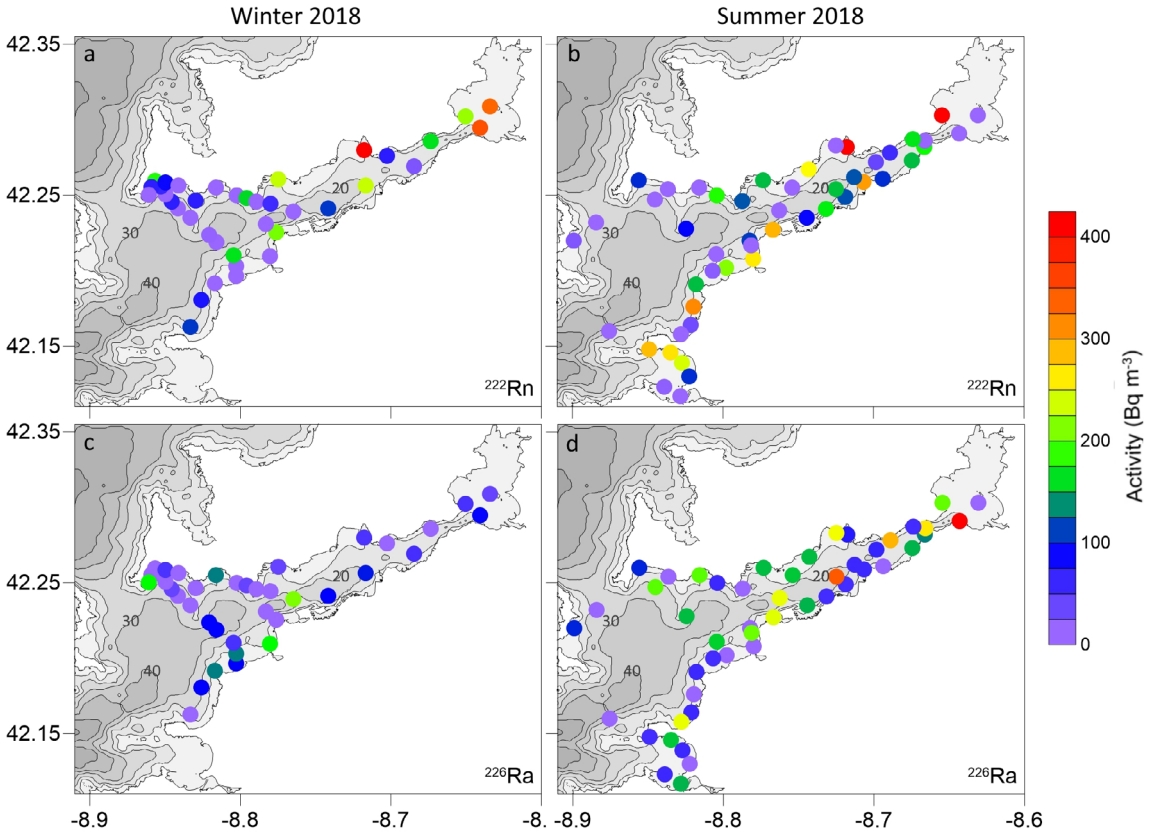

Fig 7. Spatial distribution of ^{222}Rn in excess (upper panels) and ^{226}Ra levels (lower panels) found in surface waters of the Ría de Vigo during winter and summer 2018. Bathymetric labels are shown in meters.

Table 1. Radon and ^{226}Ra levels in the three main rivers discharging into the Ría de Vigo during winter and summer 2018.

			Winter		Summer	
			^{222}Rn	^{226}Ra	^{222}Rn	^{226}Ra
	Lat	Lon	10^3 Bq m^{-3}	10^3 Bq m^{-3}	10^3 Bq m^{-3}	10^3 Bq m^{-3}
Miñor	42.11	−8.77	1.8±0.0	0.20±0.01	2.5±0.1	0.00±0.00
Verdugo-Oitavén	42.34	−8.54	1.3±0.0	0.09±0.01	4.3±0.1	0.10±0.01
Lagares	42.21	−8.75	2.6±0.1	0.04±0.01	1.2±0.1	0.04±0.01

were highly variable in space, especially in the outer part of the basin (Box 3; Fig. 8). Strong seasonality in ^{222}Rn activities was also apparent, with levels almost doubling during summer-autumn from minima in winter–spring (paired *t*-test $p < 0.001$). Apart from the particularly high ^{222}Rn levels in both the well and borehole sampled in Nerga, no evident influence of the local geology was identified. Activities of ^{226}Ra measured in continental waters of the study area (<4 10^3 Bq m^{-3}, Fig. 8) were very low by comparison to the activity of ^{222}Rn in the same samples, as expected given the strong affinity of Ra for mineral surfaces at low salinities (0.11 maximum salinity recorded in the sampled groundwaters; e.g., Gonneea et al. 2008).

We developed theoretical conservative mixing lines of both radioisotopes and plotted measured activities in the embayment for comparison (Fig. 9). For freshwater endmember composition, ^{222}Rn and ^{226}Ra activities measured in the main rivers discharging into the embayment were employed, and we accepted that ^{222}Rn and ^{226}Ra activities measured in the deep-water layers of the embayment in August were representative of the seawater endmember during summer. During winter 2018, no clear seawater endmember could be identified as we did not sample the mouth of the embayment. The downwelling conditions prevalent during the winter survey meant the seawater endmember corresponded to subtropical surface waters, with no contact with the sea floor. Considering

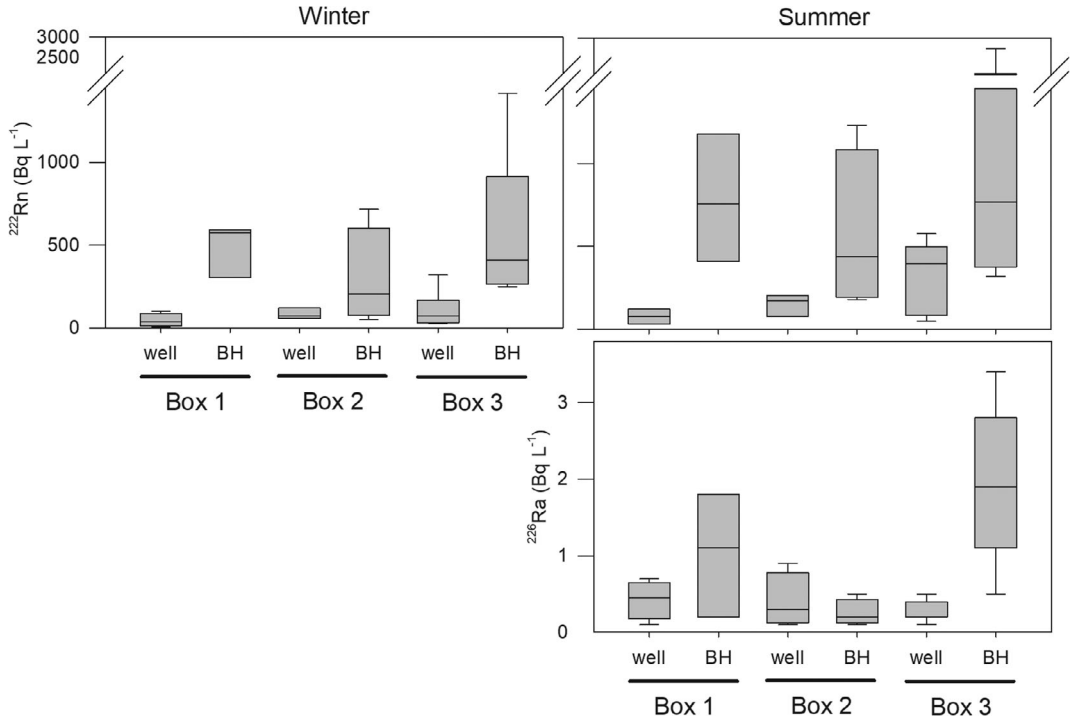

Fig 8. Box plot of the ^{222}Rn activities measured in wells (well) and boreholes (BH) in the Ría the Vigo basin during winter and summer. Data is split into the three boxes defined for the mass balance calculations. The river network was used to apportion the sub-basins to each box. Lower and upper limits of the squares represent the first and the third quartiles, the middle line represents the median of the data and whiskers are proportional to the inter-quartile range (IQR) by using 1.58 IQR/$(n)^{1/2}$.

the short half-life of ^{222}Rn (3.8 days), it is thus reasonable to assume that ^{222}Rn was absent from the seawater endmember during the winter survey. Radium has a much longer half-live (1602 years) then Rn and thus has a ubiquitous presence in seawater. Roy et al. (2018) measured ^{226}Ra in 15 sampling stations covering the entire water column and distributed along the entire GEOTRACES GA01 section (Portugal-Greenland-Canada, GEOVIDE project). Three of these stations (Sta. 1, 13, and 21) sampled the water masses along the Iberian margin. There, homogeneous, low ^{226}Ra activities (depth <800 m; 1.43 $\pm$ 0.02 Bq m^{-3}, n = 27) were associated to the Eastern North Atlantic Central Water and surface subtropical waters, i.e., those entering the Ría de Vigo during upwelling and downwelling events, respectively. We took this value for the marine ^{226}Ra endmember activity present during downwelling conditions. Under these assumptions, the distribution of measured radioisotopes with salinity deviates significantly from the theoretical conservative mixing lines for both surveys. Furthermore, several samples show radioisotope levels well in excess of the theoretical mixing line predictions, suggesting that submarine groundwater discharge can be a significant source of ^{222}Rn and ^{226}Ra to the embayment, even if other internal sources -such as diffusion from sediments or release from terrestrial suspended matter- are present in the Ría de Vigo.

Whole-system radiotracer budgets

The distribution pattern of spatially averaged ^{222}Rn inventories (i.e., the vertically integrated ^{222}Rn activities) was similar for both surveys, with the highest inventories found in the innermost sections of the embayment and the lowest in Box 3. Radium inventories increased toward the external box during winter but were comparably high within the two internal boxes during summer. In this case, ^{226}Ra inventories in the two internal boxes were higher in summer than in winter (Table 2). In all cases, the individual uncertainty associated with spatially radioisotope averaged activity values and inventories calculated from Monte Carlo simulations were lower than 15% (Table 2).

To close the radioisotope mass balances, we assume that the radionuclide content of the seawater entering the embayment during the winter survey is equal to the seawater endmember composition considered for Fig. 8. The high residual advective fluxes were the dominant terms in our mass balances (Fig. 10) and determined short residence times for each water layer (<2 days; Table 2). By comparison, turbulent mixing fluxes of ^{222}Rn, calculated in the two-layer boxes (Boxes 2 and 3) for the summer survey data were one order of magnitude lower, and comparable in magnitude to the decay and outgassing flux terms. River influxes were significant during winter but of lower magnitude during summer. Diffusive

Table 2. Results of ^{222}Rn and ^{226}Ra inventories (± associated uncertainties calculated from Monte Carlo simulations) and resulting radioisotope flux attributable to submarine groundwater discharge for the upper water layer of the three-box model of the Ría de Vigo during winter and summer 2018. Residence time refers to the estimated time needed to renew the volume of each box layer with the imposed advective rates.

		Winter 2018			Summer 2018		
		Box 1	Box 2	Box 3	Box 1	Box 2	Box 3
Residence time (h)		38±10	48±1	16±3	41±10	25±2	14±2
Inventory (Bq m^{-2})	^{222}Rn	1659±138	1172±64	471±34	998±135	779±30	458±22
	^{226}Ra	372±39	558±36	620±40	785±92	798±35	512±31
Submarine groundwater discharge (10^3 Bq s^{-1})	^{222}Rn	45±25	341±57	435±83	55±12	295±49	194±184
	^{226}Ra	13±9	49±24	437±60	38±14	137±93	−134±142

fluxes had very low relative expression (Fig. 9), equivalent to a maximum value of 4.5 ± 0.3 Bq m^{-2} d^{-1} calculated for Box 1 during the summer, in accordance with the large boxes water volume and the limited contact of the surface water layers with the sediments in Boxes 2 and 3, restricted to the shores. Similar results were obtained for the ^{226}Ra mass balances, although in this case the decay and river flux terms were of much lower importance when compared to ^{222}Rn, as expected.

The radioisotope mass balances revealed a large flux of both ^{222}Rn and ^{226}Ra in the Ría de Vigo that can be attributed to submarine groundwater discharge (Table 2). A local exception may be the flux results for Box 3 during the summer. In this case the large advective fluxes, together with sparse data in depth, which would be relevant to better accommodate the upwelling conditions that were prevalent before the survey, led to an estimate of unsupported ^{222}Rn and ^{226}Ra flux with very high associated uncertainty. In addition, the high ^{226}Ra activities measured in the bottom water mass resulted in a negative imbalance within the surface water layer of this box, albeit with high associated uncertainty. Similarly, high uncertainty (almost 100% of the result in relative terms) was found linked with the net balance of ^{222}Rn in this particular box. For the remaining results, submarine groundwater discharge is the explanation for significant ^{222}Rn and ^{226}Ra imbalances. The largest imbalances were found in Box 3 during winter, followed by Box 2 and Box 1. Furthermore, while ^{222}Rn and ^{226}Ra imbalances in Box 3 were comparable in magnitude (435 ± 83 and 437 ± 60 10^3 Bq s^{-1} for ^{222}Rn and ^{226}Ra, respectively; Table 2) during winter, in Boxes 1 and 2 the unsupported ^{222}Rn was always significantly higher than ^{226}Ra. The gap between both narrowed during summer.

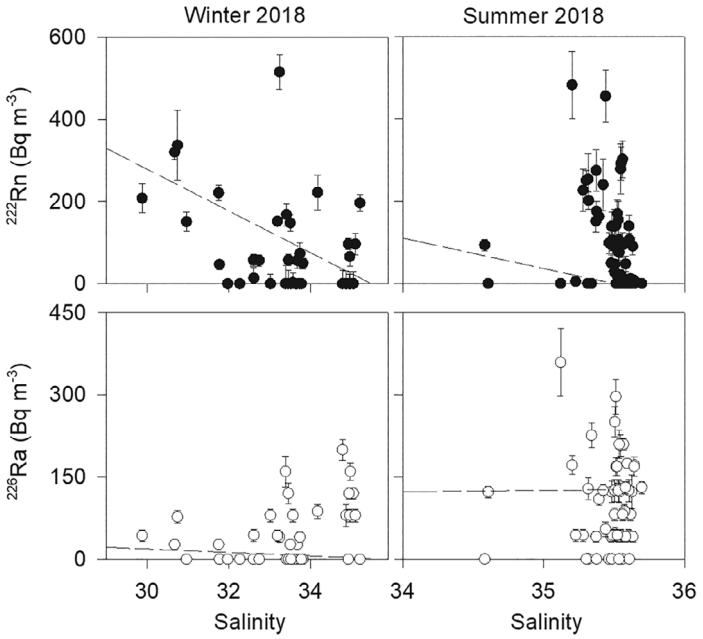

Fig 9. Distribution of excess ^{222}Rn (upper panels) and ^{226}Ra along the salinity gradient during the winter and summer surveys in surface waters of the Ría de Vigo overlain on theoretical conservative mixing lines (dashed lines).

Discussion

Radioisotope sources and sinks in a radon-prone area

Due to the high ^{238}U content of its soils and basement rocks dominated by granites (Fig. 1), the Ría de Vigo lays on the largest radon-prone area of the Iberian Peninsula. Widespread high ^{222}Rn levels, mostly measured in air, have already been linked to negative effects on local population health (e.g., López-Abente et al. 2018). The very high ^{222}Rn levels measured in groundwater samples, at least one order of magnitude higher than in continental surface waters (Fig. 8; Table 1) are therefore quite predictable. The positive depth gradient in ^{222}Rn activities is confirmed by the borehole data, where radon levels were much higher than those found in traditional wells. Aquifer specific storage, estimated through pumping tests and modeling, shows contrasting vertical values in the study area ranging from 0.013 in the regolith that feeds dug wells to 0.00032 in boreholes screened in the fractured rock (Raposo et al. 2012 and references therein).

These two distinct aquifer layers also show contrasting water transmissivities: this is two orders of magnitude higher in the regolith than within the underlying fractured rock (15 m^2 d^{-1} in the former and 0.5 m^2 d^{-1} in the latter; Soriano and Samper 2000). Therefore, groundwater flowing through the fractured rock subunit, which feeds the sampled boreholes, has a larger contact surface and higher contact time with the aquifer matrix, due to lower matrix porosity and longer groundwater residence times. This might explain the differences in ^{222}Rn activities observed for both units. In any case, the resulting large freshwater–seawater ^{222}Rn activity gradient facilitates the detection of groundwater discharge into the Ría de Vigo.

Flow through permeable sediments can drive solute transport at orders of magnitude higher rates than diffusion alone (e.g., Boudreau et al. 2001). For the surface water layers of the Ría de Vigo, contact with the sediments is restricted to the marginal shoreline, making ^{222}Rn transport by diffusion into this compartment insignificant compared to the other transport terms considered in our radioisotope budgets (Fig. 10). Riverine transport and internal decay are significant terms in our ^{222}Rn mass balances for Box 1, the smallest and shallowest of the three boxes and where the main rivers discharge. These terms lose importance in the other two boxes as advective transport increases. Even if turbulent mixing was absent from our winter mass balances, the results obtained during summer suggest that this mechanism makes a minor contribution to the overall radioisotope budget. Using turbulent mixing flux magnitudes reported by Álvarez-Salgado et al. (2000) for downwelling conditions in the Ría de Vigo (*see* Methods section) and assuming the absence of radioisotopes from the bottom water layer, this component of the mass balances would

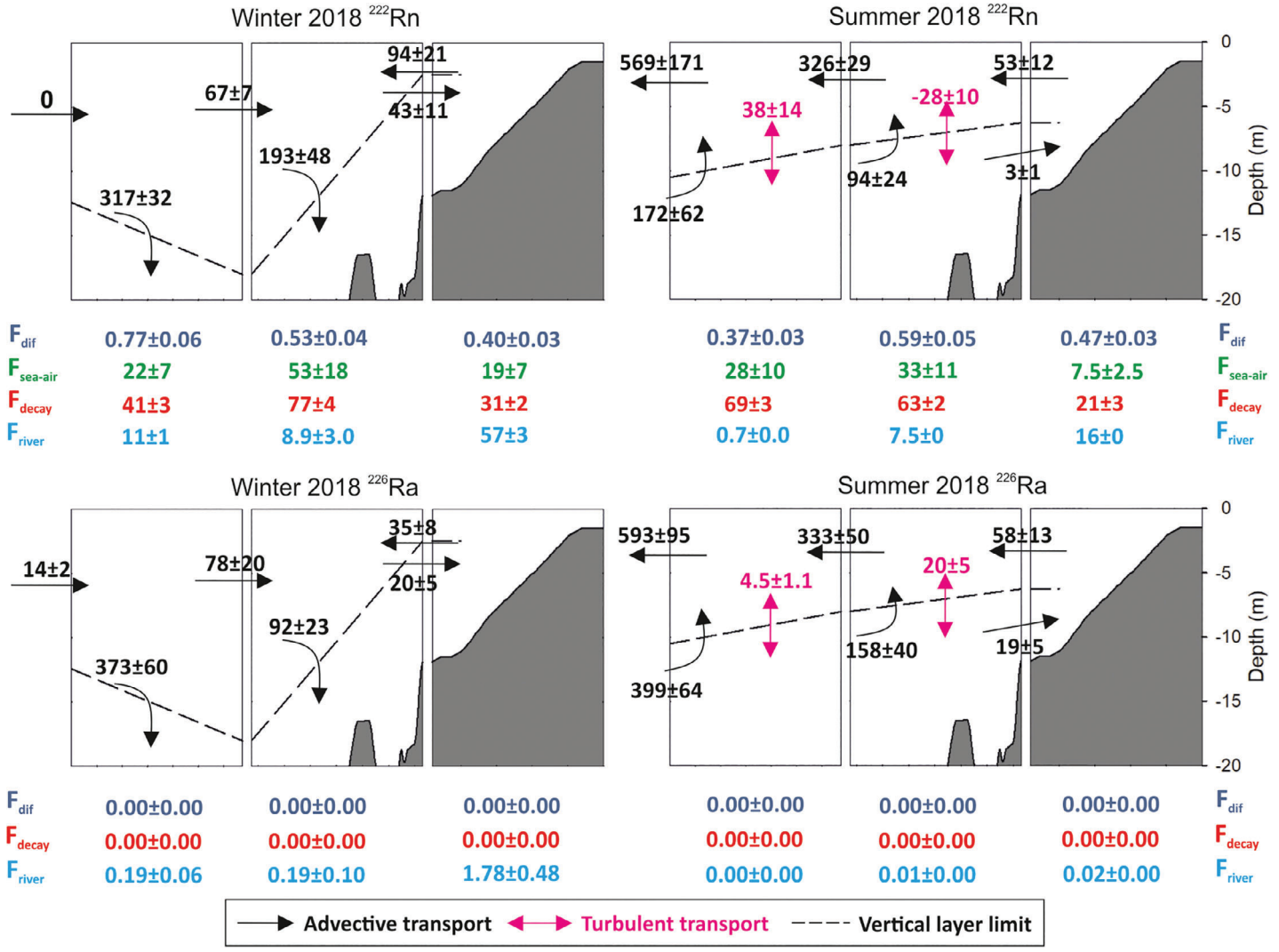

Fig 10. Schematic view of the advective and turbulent (only during summer) fluxes of ^{222}Rn in excess and ^{226}Ra calculated for the two surveys in the Ría de Vigo. Sea-air ^{222}Rn fluxes ($F_{sea\text{-}air}$, in green), radioisotope decay (F_{decay}, in red), diffusive (F_{dif}, in dark blue), and riverine (F_{river}, in light blue) fluxes are also shown. Fluxes are expressed as 10^3 Bq s^{-1}.

remain in the order of 10^4 Bq s^{-1}. Even in this extreme scenario, turbulent fluxes would make a contribution to the radioisotope mass balances in Boxes 2 and 3 that would be at least one order of magnitude lower than the advective fluxes. By comparison to the magnitude of the radioisotope imbalance within the two vertically-layered boxes that we attribute to submarine groundwater discharge, it is clear that turbulent mixing would only have a possible and measurable impact over the results obtained for ^{226}Ra in Box 2 (Table 2). During downwelling, the absence of ^{226}Ra from the bottom water mass that dominates our winter survey is nevertheless highly unlikely, because of the advective transport of ^{226}Ra from the surface water layer and the large half-life of this radioisotope. Thus, the absence of a turbulent mixing term from the winter mass balances should have very limited impact on our estimates.

Relatively low activities of ^{226}Ra were found in both groundwater and continental surface waters, which is consistent with its low solubility at low salinities. Thus, freshwater transport of dissolved ^{226}Ra to the embayment is low. Even so, surface waters can transport particles in suspension with surface-bound ^{226}Ra that would desorb when salinity increases as a result of mixing with marine waters. The Ría de Vigo does not receive high watershed suspended particle loading, also because its largest contributing river (roughly 70% of the total river discharge into the system), the Verdugo-Oitavén (Figs. 1, 3), is dammed. Here, suspended particle loads of about 3.5 mg L^{-1} were estimated before (Perez-Arlucea et al. 2005). Assuming that these particles have a ^{226}Ra content that is similar to that of the embayment's sediments (0.9 Bq kg^{-1} sediment) and that the totality of this radium would be desorbed upon mixing with seawater, the theoretical ^{226}Ra fluxes associated with particle transport into the embayment by the Verdugo-Oitavén river system during winter would be less than 0.1 Bq s^{-1}. This value is several orders of magnitude lower than the advective ^{226}Ra fluxes calculated within the embayment (Fig. 10). Another indication of the minor contribution of suspended particle-bound ^{226}Ra to ^{226}Ra budgets in the Ría de Vigo comes from the results obtained in our surveys. Despite the low river discharge and stable hydrodynamic conditions (i.e., steady upwelling forcing, low wave energy) during the summer survey compared to winter, ^{226}Ra inventories (i.e., vertically integrated ^{226}Ra activities) during summer are higher than those estimated in winter, particularly in the innermost segment of the embayment where surface continental runoff is highest.

The continental shelf is a significant source of ^{226}Ra to the embayment due to the high volume of water exchanged with the ocean and the long half-life of this radioisotope. In the Iberian margin, the Eastern North Atlantic Central Waters and subtropical surface waters that enter the embayment during upwelling and downwelling events, respectively, are characterized by homogeneous ^{226}Ra levels (1.43 ± 0.02 Bq m^{-3}) that spread significantly offshore and along the water column (Roy et al. 2018). Nevertheless, during our summer survey, ^{226}Ra levels increased significantly at the mouth of the embayment in association with the upwelled waters (>100 Bq m^{-3}). Such high ^{226}Ra levels were never detected previously, including during the GEOTRACES GA01 section that sampled the main oceanic water masses of the Iberian margin (Roy et al. 2018). These authors used optimum multiparameter analysis to identify the main processes (mixing vs. non-conservative processes) that would explain ^{226}Ra activities measured in situ. They found that the low ^{226}Ra activities characteristic of the Eastern North Atlantic Central Waters and surface subtropical waters could be explained by mixing alone. These water masses remain near the surface offshore and thus are not affected by sedimentary ^{226}Ra inputs. The large ^{226}Ra activities measured in these waters as they move into the Ría de Vigo during the summer upwelling event suggest however that the ^{226}Ra enrichment occurred prior to entering the embayment. It is well known that Eastern North Atlantic Central Water (~150–200 m depth) enters the embayment fertilizing the system during upwelling events, and that it strongly interacts with shelf sediments, developing energetic bed forms and, in combination with waves, promoting high shear stress, sediment resuspension (Villacieros-Robineau et al. 2019) and therefore, porewater exchange. In fact, indirect evidence suggests that a large proportion of the nutrient load carried by this water mass originates within the continental shelf, rather than in deeper waters offshore (Álvarez-Salgado et al. 1997). These high ^{226}Ra activities measured in the upwelled water as it enters the embayment might yet reveal the contribution of strong seawater recirculation (saline submarine groundwater discharge, sensu Burnett et al. 2003) within the adjacent shelf.

The large positive ^{226}Ra imbalances found in the two inner compartments of our model suggest additional sources of ^{226}Ra to the system that are attributable to submarine groundwater discharge, notwithstanding the large amount of ^{226}Ra entering the embayment during summer. This was not the case in the outer box, where our mass balance resulted in a deficit of ^{226}Ra in the upper water layer (Table 2). Radium levels in the bottom waters at the southern mouth station were also much higher than in the other two inner stations where we measured the vertical distribution of ^{226}Ra (Fig. 5). These results suggest that in Box 3, our steady state assumption may not be fulfilled due to the very short water residence time (Table 2), the direct exposure to the short time scale upwelling or downwelling events in the adjacent shelf, the complex 3-dimensional circulation patterns that may not be fully captured with the parameterization used (Gilcoto et al. 2017) and the large water volume of this outer box. Contrastingly, the inner parts of the embayment, more away from the continental shelf, are characterized by a lower magnitude and variability of the residual water circulation (Álvarez-Salgado et al. 2000). Despite the different origin and nature of the two radioisotopes used here (i.e., contrasting half-life times, degassing affecting only the ^{222}Rn budgets) mass balance results performed in the two inner boxes showed high

complementary coherence. Thus, our steady state assumption seems sufficient to describe radioisotope budgets in the inner parts of the embayment.

Recirculated seawater vs. fresh groundwater in submarine groundwater discharge

One of the largest sources of uncertainty in radiotracer-based submarine groundwater discharge estimates is associated with the characterization of mixing endmembers (e.g., Sadat-Noori et al. 2015). Both continental groundwater and seawater recirculating through sediment beds contribute to the overall submarine groundwater discharge flux. These two inputs have contrasting radioisotope signatures, particularly on a radon prone area as the one studied here, which adds to the variability associated with an already heterogeneous ^{222}Rn availability in continental groundwaters (e.g., Girault et al. 2016). Based on the very low ^{226}Ra content of continental groundwaters, it seems reasonable to assume that the entire ^{226}Ra budget for the Ría de Vigo is essentially associated with saline groundwater discharge. Apart from the dissolved ^{226}Ra levels found in the sampled saline groundwaters, subterranean estuaries (i.e., the underground mixing zone between continental groundwaters and infiltrating seawater; Moore 1999) can contribute to the overall ^{226}Ra budget due to ^{226}Ra mobilization caused by increased salinity. To estimate the ^{226}Ra content of the saline endmember within the Ría de Vigo, we used the sampled saline groundwaters together with ^{226}Ra levels measured in two contrasting subterranean estuaries within the embayment (Calvo-Martin et al. 2021). Samples from these subterranean estuaries that presented ^{222}Rn activities below those at sediment–porewater equilibrium, indicative of recent seawater infiltration, were excluded from this estimation. We can then use the dissolved ^{226}Ra (688 ± 15 Bq m^{-3}, including the subterranean estuaries) and ^{222}Rn in excess (919 ± 241 Bq m^{-3}) activities determined in embayment sediment groundwaters to estimate the contribution made by saline submarine groundwater discharge to the total ^{222}Rn in excess budget. The remaining ^{222}Rn in excess imbalance can thus by attributed to fresh submarine groundwater discharge. This gives us a ^{222}Rn input linked to fresh submarine groundwater discharge of 27 ± 23 and 3.8 ± 1.5 Bq s^{-1} in Box 1 and 277 ± 97 and 112 ± 37 Bq s^{-1} in Box 2 during winter and summer, respectively. Radon and ^{226}Ra mass balances are effectively equivalent in Box 3 for both periods. This allows us to advance the first estimate of fresh submarine groundwater discharge to the Ría de Vigo.

Taking into account the hydrogeology of the local aquifers and the ^{222}Rn activities measured in continental groundwaters of the basin, two different fresh groundwater endmembers can be considered for a mixing model: those within the upper aquifer layers (regolith) and those contained within the deeper fractured rock. If we consider the average ^{222}Rn activities in the regolith aquifer unit as representative of the continental groundwater endmember for each box, the volumetric discharge of fresh groundwater into the Ría de Vigo would be 3.72 ± 1.73 m^3 s^{-1} during winter (3.28 ± 1.32 m^3 s^{-1} into Box 2 and 0.45 ± 0.41 m^3 s^{-1} into Box 1) and 0.63 ± 0.26 m^3 s^{-1} during summer (0.58 ± 0.24 m^3 s^{-1} into Box 2 and 0.05 ± 0.03 m^3 s^{-1} into Box 1). If instead we use the average ^{222}Rn activities from the sampled boreholes (screened at the fractured rock aquifer) for each box, then the volumetric discharge into the embayment would be 1.01 ± 0.55 m^3 s^{-1} during winter (0.95 ± 0.50 m^3 s^{-1} into Box 2 and 0.06 ± 0.05 m^3 s^{-1} into Box 1) and 0.21 ± 0.13 m^3 s^{-1} during summer (0.21 ± 0.13 m^3 s^{-1} into Box 2 and 0.01 ± 0.00 m^3 s^{-1} into Box 1).

The surface aquifer unit contained in crystalline rocks and within the regolith has three orders of magnitude higher volumetric water storage capacity than the fractured bedrock underneath. The surface unit also has higher recharge/discharge rates and lateral transmissivities by several orders of magnitude (Mota et al. 2004; Ramalho et al. 2012; Raposo et al. 2012). Thus, the groundwater contained within the regolith is most likely to be the dominant continental groundwater endmember in fresh submarine groundwater discharge into the Ría de Vigo. The estimated groundwater discharge originating from the surface aquifer layers are equivalent to 0.43 ± 0.40 and 0.90 ± 0.36 cm d^{-1} in Box 1 and Box 2 during winter, respectively and 0.05 ± 0.02 and 0.16 ± 0.06 cm d^{-1} in Box 1 and Box 2 during summer, assuming uniform areal distribution for each box. Both volumetric and advective discharge estimates fall within the range of previous submarine groundwater discharge studies in temperate estuaries (Santos et al. 2010; Rocha et al. 2016; Petermann et al. 2018). Furthermore, extrapolating our results on an annual basis and using the maximum recharge of Galician crystalline aquifers determined by Raposo et al. (2012), our fresh groundwater discharge estimates represent 10% of the total maximum groundwater recharge for the basin. Using the parametrization of Galician aquifer recharge based on rainfall (Raposo et al. 2012) and the annual precipitation over the basin for the 2017–2018 hydrological year, this contribution rises to 20%. Although these numbers should be taken with caution given the large extrapolations, they confirm how reasonable our discharge magnitudes are. Moreover, these submarine groundwater discharge estimates should be taken as representative of the lower end of the range of potential discharge rates to the Ría de Vigo because we did not assess potential continental groundwater discharge into the deeper water layers of the embayment or the groundwater ^{222}Rn loss by decay during the time span separating discharge and our records (e.g., Petermann et al. 2018).

Seawater recirculation through marine sands and coastal aquifers is a major component of submarine groundwater discharge worldwide (Kwon et al. 2014). Our data suggests the contribution of the continental source term to the overall ^{226}Ra flux estimates associated with submarine groundwater discharge into the Ría de Vigo is minimal ($<10^3$ Bq s^{-1}). Given the low solubility of ^{226}Ra at low salinities, we can use the ^{226}Ra flux associated with submarine groundwater discharge calculated by our mass balances to develop a first estimate of

the volumetric magnitude of seawater recirculation through the benthic compartment in the Ría de Vigo. Assuming a saline groundwater endmember ^{226}Ra composition equal to that determined in the saline groundwaters and subterranean estuaries of the embayment and then correcting for the flux of ^{226}Ra associated with continental groundwater, seawater recirculation rates for Box 1 and Box 2 are estimated at 18.3 ± 13.0 and 65.9 ± 33.0 m^3 s^{-1} during winter, respectively. These figures would imply that the entire volume of the surface seawater within the Ría de Vigo is flushed through the (permeable) seafloor in 39 ± 28 and 62 ± 31 days for Boxes 1 and 2, respectively. If we consider the ^{226}Ra fluxes computed for the summer period, the volume of the surface layer of the Ría de Vigo would recirculate through local permeable seabeds in 13 ± 5 and 21 ± 14 days in Box 1 and Box 2, respectively. During summer, the lower hydraulic gradients within the coastal aquifers would facilitate seawater intrusion, which would promote desorption and thus large fluxes of radium to the overlying waters, contributing in this way to the apparently higher ^{226}Ra fluxes we associated with submarine groundwater discharge. As such, our estimates for the summer should be taken with caution until the drivers of seasonal endmember variability are better resolved.

Conclusions

This study provides the first estimates of submarine groundwater discharge to the Ría de Vigo, a highly productive coastal ecosystem of major environmental and economic significance. Our analysis includes an explicit representation of the circulation patterns inside the embayment to account for the seasonality of local water flows, coupled with a dual isotope approach. This combined approach permits the quantitative distinction between fresh and saline submarine groundwater discharge, based on (i) the complementary relationship of ^{222}Rn and ^{226}Ra, its parent isotope, (ii) the comparatively low ^{226}Ra content of continental groundwaters, and (iii) the sensitivity of ^{226}Ra adsorption to salinity. Although coastal basins dominated by crystalline aquifers have reduced groundwater storage capacity and therefore are thought to support low fresh submarine groundwater discharge rates, the vertical extension of the regolith and the secondary porosity of the basement rocks associated with the presence of faults and fractures may explain the significant fresh submarine groundwater discharge rates reported here.

The volumetric groundwater discharge into the system, calculated to originate in the surface aquifer unit, equates to $9\% \pm 4\%$ and $23\% \pm 9\%$ of the estimated total river discharge into the embayment during winter and summer, respectively. Whether or not this translates into significant terrestrially derived solute loading is yet to be seen. Nevertheless, our discharge estimates are compartmentalized into different sectors, hence offering a degree of spatial discrimination of both the continental endmember composition and the magnitude of the discharge of continental groundwaters into the embayment. Our ^{222}Rn measurements within the embayment generally showed spatial correlation of enrichments with the location of prevailing faults and fluvial deposits, which in effect maps out potential preferential discharge sites; this information can be used in support of spatial management and water security policies within the embayment. Nevertheless, we note that groundwater source attribution is still needed to confirm the origin and magnitude of our estimated continental groundwater discharge rates.

Our combined tracer and mass balance approach also highlighted the potential role of the permeable seabed to the biogeochemistry of the system. These sediments cover 58% of the embayment's benthic compartment and are the dominant texture in the adjacent continental shelf. Large seawater recirculation rates are clearly apparent from our study, which implies that permeable sediment biogeochemistry has the potential to be a crucial component in the cycling of dissolved chemicals even in such a highly productive system as the Ría de Vigo. This matter deserves further attention, considering the changes expected to this eastern boundary upwelling ecosystem in the future, in order to support the resilience and carrying capacity of the Ría de Vigo and preserve its ecological and economic value.

References

Álvarez-salgado, X. A., C. G. Castro, F. F. Pérez, and F. Fraga. 1997. Nutrient mineralization patterns in shelf waters of the Western Iberian upwelling. Cont. Shelf Res. **17**: 1247–70. doi:10.1016/S0278-4343(97)00014-9

Álvarez-Salgado, X. A., J. Gago, B. M. Míguez, M. Gilcoto, and F. F. Pérez. 2000. Surface waters of the NW Iberian margin: Upwelling on the shelf versus outwelling of upwelled waters from the Rías Baixas. Estuar. Coast. Shelf Sci. **51**: 821–37. doi:10.1006/ecss.2000.0714

Arístegui, J., et al. 2009. Sub-regional ecosystem variability in the canary current upwelling. Prog. Oceanogr. **83**: 33–48. doi:10.1016/j.pocean.2009.07.031

Bakun, A. 1973. Coastal upwelling indices, west coast of North America, 1946–71. U.S. Dep. Commer., NOAA Tech. Rep., NMFS SSRF-671.

Boudreau, B. P., and others. 2001. Permeable marine sediments: Overturning an old paradigm. EOS Trans. Am. Geophys. Union **82**: 133–7.

Burnett, W. C., H. Bokuniewicz, M. Huettel, W. S. Moore, and M. Taniguchi. 2003. Groundwater and pore water inputs to the coastal zone. Biogeochemistry **66**: 3–33. doi:10.1023/B:BIOG.0000006066.21240.53

Calvo-Martin, E., X. A. Álvarez-Salgado, C. Rocha, and J. S. P. Ibánhez. 2021. Reactive solute transport through two contrasting subterranean estuary exit sites in the Ría de Vigo (NW Iberian Peninsula). Front. Mar. Sci. **8**: 626813. doi:10.3389/fmars.2021.626813

Cho, H.-M., G. Kim, E. Y. Kwon, N. Moosdorf, J. Garcia-Orellana, and I. R. Santos. 2018. Radium tracing nutrient inputs through submarine groundwater discharge in the global ocean. Sci. Rep. **8**: 2439. doi:10.1038/s41598-018-20806-2

Colbert, S. L., and D. E. Hammond. 2008. Shoreline and seafloor fluxes of water and short-lived Ra isotopes to surface water of San Pedro Bay, CA. Mar. Chem. **108**: 1–17. doi:10.1016/j.marchem.2007.09.004

Des, M., M. deCastro, M. C. Sousa, J. M. Dias, and M. Gómez-Gesteira. 2019. Hydrodynamics of river plume intrusion into an adjacent estuary: The Minho River and Ria de Vigo. J. Mar. Syst. **189**: 87–97. doi:10.1016/j.jmarsys.2018.10.003

FAO. 2018. The state of world fisheries and aquaculture 2018—meeting the sustainable development goals. Rome. Licence: CC BY-NC-SA 3.0 IGO.

Fernández, E., X. A. Álvarez-Salgado, R. Beiras, A. Ovejero, and G. Méndez. 2016. Coexistence of urban uses and shellfish production in an upwelling-driven, highly productive marine environment: The case of the Ría de Vigo (Galicia, Spain). Reg. Stud. Mar. Sci. **8**: 362–70. doi:10.1016/j.rsma.2016.04.002

Figueiras, F. G., U. Labarta, and M. J. Fernández Reiriz. 2002. Coastal upwelling, primary production and mussel growth in the Rías Baixas of Galicia. Hydrobiologia **484**: 121–31. doi:10.1023/A:1021309222459

García-García, A., S. García-Gil, and F. Vilas. 2005. Quaternary evolution of the Ría de Vigo, Spain. Mar. Geol. **220**: 153–79. doi:10.1016/j.margeo.2005.06.015

Gilcoto, M., and others. 2017. Rapid response to coastal upwelling in a semienclosed bay. Geophys. Res. Lett. **44**: 2388–97. doi:10.1002/2016GL072416

Girault, F., F. Perrier, and T. A. Przylibski. 2016. Radon-222 and radium-226 occurrence in water: A review. Geol. Soc. London, Spec. Publ. **451**: SP451.3.

Gonneea, M. E., P. J. Morris, H. Dulaiova, and M. A. Charette. 2008. New perspectives on radium behavior within a subterranean estuary. Mar. Chem. **109**: 250–67. doi:10.1016/j.marchem.2007.12.002

Gustafson, G., and J. Krásný. 1994. Crystalline rock aquifers: Their occurrence, use and importance. Appl. Hydrogeol. **2**: 64–75. doi:10.1007/s100400050051

IGME, Instituto Geológico y Minero de España. 2003. Mapa Geológico de España 1:50000 (MAGNA50). Pages 185, 186, 222, 223, 224, 260, 261, and 262.

Johannes, R. E. 1980. The ecological significance of the submarine discharge of groundwater. Mar. Ecol. Prog. Ser. **3**: 365–73.

Kwon, E. Y., et al. 2014. Global estimate of submarine groundwater discharge based on an observationally constrained radium isotope model. Geophys. Res. Lett. **41**(23): 8438–8444. doi:10.1002/2014GL061574

Labarta, U., and M. J. Fernández-Reiriz. 2019. The Galician mussel industry: Innovation and changes in the last forty years. Ocean Coast. Manag. **167**: 208–18. doi:10.1016/j.ocecoaman.2018.10.012

Lecher, A. L., K. Mackey, R. Kudela, J. Ryan, A. Fisher, J. Murray, and A. Paytan. 2015. Nutrient loading through submarine groundwater discharge and phytoplankton growth in Monterey Bay, CA. Environ. Sci. Technol. **49**: 6665–73. doi:10.1021/acs.est.5b00909

Leote, C., J. Ibánhez, and C. Rocha. 2008. Submarine groundwater discharge as a nitrogen source to the Ria Formosa studied with seepage meters. Biogeochemistry **88**: 185–94. doi:10.1007/s10533-008-9204-9

López-Abente, G., O. Núñez, P. Fernández-Navarro, J. M. Barros-Dios, I. Martín-Méndez, A. Bel-Lan, J. Locutura, L. Quindós, C. Sainz, and A. Ruano-Ravina. 2018. Residential radon and cancer mortality in Galicia, Spain. Sci. Total Environ. **610–611**: 1125–32. doi:10.1016/j.scitotenv.2017.08.144

Luijendijk, E., T. Gleeson, and N. Moosdorf. 2020. Fresh groundwater discharge insignificant for the world's oceans but important for coastal ecosystems. Nat. Commun. **11**: 1–12. doi:10.1038/s41467-020-15064-8

Luo, X., J. J. Jiao, Y. Liu, X. Zhang, W. Liang, and D. Tang. 2018. Evaluation of water residence time, submarine groundwater discharge, and maximum new production supported by groundwater borne nutrients in a coastal upwelling shelf system. J. Geophys. Res. Oceans **123**: 631–55. doi:10.1002/2017JC013398

MacIntyre, S., R. Wanninkhof, and J. P. Chanton. 1995. Trace gas exchange across the air–water interface in freshwater and coastal marine environments. In P. A. Matson and R. C. Hariss [eds.], Biogenic trace gases: Measuring emissions from soil and water. Blackwell Science, 52–97.

Martens, C. S., G. W. Kipphut, and J. V. Klump. 1980. Sediment–water chemical exchange in the coastal zone traced by in situ Radon-222 flux measurements. Science **208**: 285–8. doi:10.1126/science.208.4441.285

Moore, W. S. 1999. The subterranean estuary: A reaction zone of ground water and sea water. Mar. Chem. **65**: 111–25. doi:10.1016/S0304-4203(99)00014-6

Moore, W. S. 2010. The effect of submarine groundwater discharge on the ocean. Ann. Rev. Mar. Sci. **2**: 59–88. doi:10.1146/annurev-marine-120308-081019

Mota, R., F. A. Monteiro Santos, A. Mateus, F. O. Marques, M. A. Gonçalves, J. Figueiras, and H. Amaral. 2004. Granite fracturing and incipient pollution beneath a recent landfill facility as detected by geoelectrical surveys. J. Appl. Geophys. **57**: 11–22. doi:10.1016/j.jappgeo.2004.08.007

Perez-Arlucea, M., G. Mendez, F. Clemente, M. Nombela, B. Rubio, and M. Filgueira. 2005. Hydrology, sediment yield, erosion and sedimentation rates in the estuarine environment of the Ria de Vigo, Galicia, Spain. J. Mar. Syst. **54**: 209–26. doi:10.1016/j.jmarsys.2004.07.013

Petermann, E., K. Knöller, C. Rocha, J. Scholten, R. Stollberg, H. Weiß, and M. Schubert. 2018. Coupling end-member mixing analysis and isotope mass balancing (222-Rn) for

differentiation of fresh and Recirculated submarine groundwater discharge into Knysna estuary, South Africa. J. Geophys. Res. Oceans **123**: 952–70. doi:10.1002/2017JC013008

Ramalho, E. C., J. P. Carvalho, R. Gonçalves, and F. A. Monteiro Santos. 2012. Understanding the 3D structure of a thermal water fissured granite aquifer by use of geophysical studies. Pure Appl. Geophys. **169**: 2031–46. doi:10.1007/s00024-012-0456-x

Raposo, J. R., J. Molinero, and J. Dafonte. 2012. Parameterization and quantification of recharge in crystalline fractured bedrocks in Galicia-Costa (NW Spain). Hydrol. Earth Syst. Sci. **16**: 1667–83. doi:10.5194/hess-16-1667-2012

Raposo, J. R., J. Dafonte, and J. Molinero. 2013. Assessing the impact of future climate change on groundwater recharge in Galicia-Costa, Spain. Hydrogeol. J. **21**: 459–79. doi:10.1007/s10040-012-0922-7

Ríos, A. F., M. Á. Nombela, F. F. Pérez, G. Rosón, and F. Fraga. 1992. Calculation of runoff to an estuary. Ria de Vigo. Scientia Marina **56**: 29–33.

Rocha, C., C. Veiga-Pires, J. Scholten, K. Knoeller, D. R. Gröcke, L. Carvalho, J. Anibal, and J. Wilson. 2016. Assessing land–ocean connectivity via submarine groundwater discharge (SGD) in the Ria Formosa lagoon (Portugal): Combining radon measurements and stable isotope hydrology. Hydrol. Earth Syst. Sci. **20**: 3077–98. doi:10.5194/hess-20-3077-2016

Rosón, G., X. A. Alvarez-Salgado, and F. F. Pérez. 1997. A non-stationary box model to determine residual fluxes in a partially mixed estuary, based on both thermohaline properties: Application to the Ria de Arousa (NW Spain). Estuar. Coast. Shelf Sci. **44**: 249–62. doi:10.1006/ecss.1996.0127

Roy, E. L., et al. 2018. The ^{226}Ra–Ba relationship in the North Atlantic during GEOTRACES-GA01. Biogeosciences **15**: 3027–48. doi:10.5194/bg-15-3027-2018

Sadat-Noori, M., I. R. Santos, C. J. Sanders, L. M. Sanders, and D. T. Maher. 2015. Groundwater discharge into an estuary using spatially distributed radon time series and radium isotopes. J. Hydrol. **528**: 703–19. doi:10.1016/j.jhydrol.2015.06.056

Santos, I. R., R. N. Peterson, B. D. Eyre, and W. C. Burnett. 2010. Significant lateral inputs of fresh groundwater into a stratified tropical estuary: Evidence from radon and radium isotopes. Mar. Chem. **121**: 37–48. doi:10.1016/j.marchem.2010.03.003

Santos, I.R, B.D, Eyre, and M, Huettel. 2012. The driving forces of porewater and groundwater flow in permeable coastal sediments: A review. Estuar. Coast. Shelf Sci. **98**: 1–15. doi:10.1016/j.ecss.2011.10.024

Schubert, M., A. Paschke, E. Lieberman, and W. C. Burnett. 2012. Air–water partitioning of ^{222}Rn and its dependence on water temperature and salinity. Environ. Sci. Technol. **46**: 3905–11. doi:10.1021/es204680n

Soriano, G., and J. Samper. 2000. Hidrogeología de una pequeña Cuenca piloto en medios graníticos: Cuenca del Valiñas (A Coruña). In Las Aguas Subterráneas en el Noroeste de la Península Ibérica. Madrid: IGME.

Taniguchi, M., et al. 2019. Submarine groundwater discharge: Updates on its measurement techniques, geophysical drivers, magnitudes and effects. Front. Environ. Sci. **7**: doi:10.3389/fenvs.2019.00141

Taylor, J. 1997. Introduction to error analysis, the study of uncertainties in physical measurements, 2nd Edition. Univ. Science Books.

Vilas, F., A. M. Bernabeu, and G. Méndez. 2005. Sediment distribution pattern in the Rias Baixas (NW Spain): Main facies and hydrodynamic dependence. J. Mar. Syst. **54**: 261–76. doi:10.1016/j.jmarsys.2004.07.016

Villacieros-Robineau, N., and others. 2019. Bottom boundary layer and particle dynamics in an upwelling affected continental margin (NW Iberia). J. Geophys. Res. Oceans **124**: 9531–52. doi:10.1029/2019JC015619

Welch, E. M., H. Dulai, A. El-Kadi, and C. K. Shuler. 2019. Submarine groundwater discharge and stream baseflow sustain pesticide and nutrient fluxes in Faga'alu Bay, American Samoa. Front. Environ. Sci. **7**. doi:10.3389/fenvs.2019.00162

Wilson, A. M. 2005. Fresh and saline groundwater discharge to the ocean: A regional perspective. Water Resour. Res. **41**: W02016. doi:https://doi.org/10.1029/2004WR003399

Zhou, Y., A. H. Sawyer, C. H. David, and J. S. Famiglietti. 2019. Fresh submarine groundwater discharge to the near-global coast. Geophys. Res. Lett. **46**: 5855–63. doi:10.1029/2019GL082749

Acknowledgments

We are thankful to the crew of the Kraken boat (University of Vigo) for field support during the two sampling surveys. Field and laboratory support by V. Vieitez and M.J. Pazó are also greatly appreciated. Vertical temperature, salinity and pressure data measured in the Ría de Vigo during the 27th February 2018 was obtained from the Galician Monitoring Program (INTECMAR; www.intecmar.gal). We are thankful to three anonymous reviewers and the editor whose comments helped to improve the early version of the manuscript. This study was financed by the SUBACID project (SUBmarine groundwater discharge [SGD] impact on coastal ACIDification processes in contrasting European Atlantic Shores: toward securing ecosystem services and food production), funded by the Irish Research Council and the European Union's Horizon 2020 research and innovation programme under the Marie Skłodowska-Curie grant agreement No. 713279 through the CAROLINE program (CLNE/2017/210).

Conflict of Interest

None declared.

Submitted 24 April 2020
Revised 25 November 2020
Accepted 01 March 2021

Associate editor: Bradley Eyre